

## LETTERS

# Sphingosine-1-phosphate is a missing cofactor for the E3 ubiquitin ligase TRAF2

Sergio E. Alvarez<sup>1\*</sup>†, Kuzhuvelil B. Harikumar<sup>1\*</sup>, Nitai C. Hait<sup>1</sup>, Jeremy Allegood<sup>1</sup>, Graham M. Strub<sup>1</sup>, Eugene Y. Kim<sup>1</sup>, Michael Maceyka<sup>1</sup>, Hualiang Jiang<sup>2</sup>, Cheng Luo<sup>2</sup>, Tomasz Kordula<sup>1</sup>, Sheldon Milstien<sup>1</sup> & Sarah Spiegel<sup>1</sup>

Tumour-necrosis factor (TNF) receptor-associated factor 2 (TRAF2) is a key component in NF- $\kappa$ B signalling triggered by TNF- $\alpha$ <sup>1,2</sup>. Genetic evidence indicates that TRAF2 is necessary for the polyubiquitination of receptor interacting protein 1 (RIP1)<sup>3</sup> that then serves as a platform for recruitment and stimulation of I $\kappa$ B kinase, leading to activation of the transcription factor NF- $\kappa$ B. Although TRAF2 is a RING domain ubiquitin ligase, direct evidence that TRAF2 catalyses the ubiquitination of RIP1 is lacking. TRAF2 binds to sphingosine kinase 1 (SphK1)<sup>4</sup>, one of the isoenzymes that generates the pro-survival lipid mediator sphingosine-1-phosphate (S1P) inside cells. Here we show that SphK1 and the production of S1P is necessary for lysine-63-linked polyubiquitination of RIP1, phosphorylation of I $\kappa$ B kinase and I $\kappa$ B $\alpha$ , and I $\kappa$ B $\alpha$  degradation, leading to NF- $\kappa$ B activation. These responses were mediated by intracellular S1P independently of its cell surface G-protein-coupled receptors. S1P specifically binds to TRAF2 at the amino-terminal RING domain and stimulates its E3 ligase activity. S1P, but not dihydro-S1P, markedly increased recombinant TRAF2-catalysed lysine-63-linked, but not lysine-48-linked, polyubiquitination of RIP1 *in vitro* in the presence of the ubiquitin conjugating enzymes (E2) UbcH13 or UbcH5a. Our data show that TRAF2 is a novel intracellular target of S1P, and that S1P is the missing cofactor for TRAF2 E3 ubiquitin ligase activity, indicating a new paradigm for the regulation of lysine-63-linked polyubiquitination. These results also highlight the key role of SphK1 and its product S1P in TNF- $\alpha$  signalling and the canonical NF- $\kappa$ B activation pathway important in inflammatory, antiapoptotic and immune processes.

Engagement of the TNF receptor results in the assembly of multi-component receptor-associated signalling complexes by adaptors including TNFR1-associated death domain (TRADD), the RING domain ubiquitin ligases (such as TRAF2) and RIP1, which together activate the I $\kappa$ B kinase (IKK) complex comprising two highly homologous kinase subunits, IKK $\alpha$  (also called IKK1) and IKK $\beta$  (IKK2), and a regulatory subunit NEMO (IKK $\gamma$ ). Phosphorylation of I $\kappa$ B $\alpha$  by the IKK complex leads to its lysine 48 (Lys 48)-linked polyubiquitination and subsequent proteasomal degradation, liberating the NF- $\kappa$ B dimer—a transcription factor comprising p65 and p50 subunits—which enters the nucleus and regulates transcription of target genes<sup>1,2,5</sup>. It has been demonstrated that the interaction of SphK1 with TRAF2 and subsequent activation of SphK1 links TNF- $\alpha$  signals to the activation of NF- $\kappa$ B<sup>4</sup>, yet the mechanism of the involvement of SphK1 in the canonical NF- $\kappa$ B pathway has not been elucidated. To this end, expression of SphK1 was downregulated with small interfering RNA (siRNA), which reduced its levels by more than 70% without affecting SphK2 levels (Supplementary

Fig. 1a). Depletion of SphK1 significantly decreased TNF- $\alpha$ -stimulated phosphorylation of IKK $\alpha$ , IKK $\beta$  and I $\kappa$ B $\alpha$  (Fig. 1a), as well as NF- $\kappa$ B DNA binding and reporter activities (Supplementary Fig. 1b–d). In contrast, depletion of SphK2 had no significant effects (Supplementary Fig. 1a, d). To exclude off-target effects, SphK1 expression was also downregulated with siRNAs targeted to two other regions of the SphK1 sequence, and both inhibited TNF- $\alpha$ -induced phosphorylation of I $\kappa$ B $\alpha$  and IKK $\alpha$ / $\beta$  (Supplementary Fig. 2a). Similar results were obtained in several other cell types (Supplementary Fig. 2b), indicating that SphK1 has a general role in the canonical NF- $\kappa$ B pathway.

To demonstrate conclusively the involvement of SphK1, we also used pharmacological and genetic approaches. The specific SphK1 inhibitor SK1-I, which decreases intracellular S1P levels<sup>6</sup>, reduced TNF- $\alpha$ -induced I $\kappa$ B $\alpha$  degradation and phosphorylation of IKK $\alpha$  and IKK $\beta$  (Fig. 1b) in a dose-dependent manner that correlated with inhibition of SphK1 activity (Supplementary Fig. 3a, c); however, SK1-I did not have a significant effect on S1P-induced ERK1/2 phosphorylation (Fig. 1b), as expected for S1P triggered G-protein-coupled receptor signalling pathways<sup>7</sup>. Activation of Jun N-terminal kinase (JNK) by TNF- $\alpha$  was also diminished by depletion of SphK1 (Fig. 1a) or its inhibition (Supplementary Fig. 3b). Similarly, SK1-I reduced activation of p38 (Supplementary Fig. 3a). Finally, upon TNF- $\alpha$  treatment, phosphorylation of I $\kappa$ B $\alpha$  and IKK $\alpha$ / $\beta$  was absent in *Sphk1*<sup>-/-</sup> mouse embryonic fibroblasts (MEFs) compared with that in *Sphk1*<sup>+/+</sup> MEFs (Fig. 1c). Immunofluorescence and western blotting revealed that depletion of SphK1 diminished TNF- $\alpha$ -induced translocation of p65 and p50 from the cytosol to the nucleus (Supplementary Fig. 4a, b). Similarly, *Sphk1*<sup>-/-</sup> MEFs were also impaired in TNF- $\alpha$ -induced translocation of p65 to the nucleus, and transfection of SphK1 rescued this defect, whereas catalytically inactive SphK1 did not (Fig. 1d). Thus, SphK1 is required for TNF- $\alpha$ -induced activation of IKK $\alpha$ / $\beta$ , I $\kappa$ B $\alpha$  phosphorylation and nuclear translocation of NF- $\kappa$ B. Moreover, CD40-induced phosphorylation of IKK and I $\kappa$ B $\alpha$  in a B lymphoid cell line was attenuated by SK1-I, which reduced intracellular levels of S1P (Supplementary Fig. 5a, b). Likewise, downregulation of SphK1 also reduced phosphorylation of IKK and I $\kappa$ B $\alpha$  by phorbol 12-myristate 13-acetate (PMA) and ionomycin stimulation (Supplementary Fig. 5c), supporting the general importance of SphK1 in NF- $\kappa$ B activation.

Activation of SphK1 typically results in the spatially restricted formation and secretion of S1P that acts in an autocrine or paracrine manner to activate its G-protein-coupled receptors on the cell surface<sup>7</sup>. As S1P<sub>1</sub> and S1P<sub>3</sub> receptors may activate NF- $\kappa$ B through G protein signalling<sup>8,9</sup>, it was important to determine whether 'inside-out signalling' by S1P could be responsible for SphK1-dependent activation of NF- $\kappa$ B. In agreement with previous studies<sup>4,10,11</sup>, TNF- $\alpha$  activated

<sup>1</sup>Department of Biochemistry and Molecular Biology and the Massey Cancer Center, Virginia Commonwealth University School of Medicine, 1101 E. Marshall Street, Richmond, Virginia 23298, USA. <sup>2</sup>State Key Laboratory of Drug Research, Shanghai Institute of Materia Medica, Chinese Academy of Sciences, Shanghai 201203, China. †Present address: IMIBIO-SL CONICET, Ejército de los Andes 950, San Luis 5700, Argentina.

\*These authors contributed equally to this work.

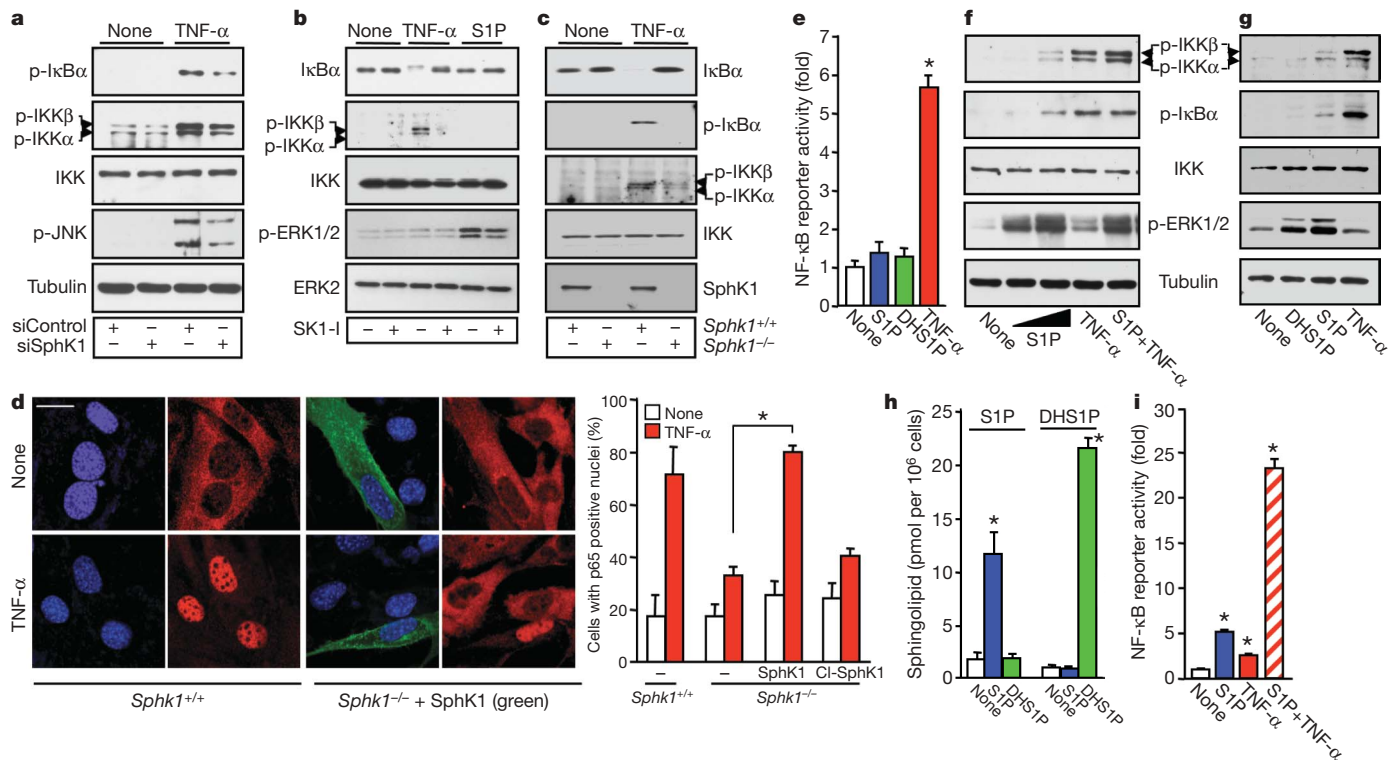


**Figure 1 | SphK1 and intracellular S1P are necessary for NF- $\kappa$ B activation by TNF- $\alpha$  independently of S1P receptors.** **a**, HEK 293 cells transfected with siControl or siSphK1 were treated with TNF- $\alpha$  and analysed by immunoblotting. **b**, A7 cells were pre-treated with SK1-I (10  $\mu$ M) and stimulated with TNF- $\alpha$  or S1P (100 nM). **c**, *Sphk1*<sup>+/+</sup> and *Sphk1*<sup>-/-</sup> MEFs were stimulated with TNF- $\alpha$ . **d**, *Sphk1*<sup>+/+</sup> or *Sphk1*<sup>-/-</sup> MEFs transfected with V5-SphK1 or catalytically inactive SphK1 (G82D) (CI-SphK1) were treated with TNF- $\alpha$ , stained with Hoechst (blue), and p65 (red) and V5 (green) antibodies, and visualized by confocal microscopy. Scale bar, 20  $\mu$ m. Percentages of cells with p65 positive nuclei are shown. \* $P$  < 0.01. **e**, NF- $\kappa$ B

SphK1 (Supplementary Fig. 6a,b), increased the intracellular mass levels of S1P and enhanced its transport out of cells (Supplementary Fig. 6c). However, 100 nM of exogenously added S1P or dihydro-S1P, which only lacks the double bond in S1P and binds to and activates all of the S1P receptors<sup>7</sup>, did not have any detectable effects on phosphorylation of I $\kappa$ B $\alpha$  or its degradation, nor did they stimulate IKK phosphorylation in A7, HEK 293 or HeLa cells (Fig. 1b, f, g and Supplementary Fig. 6d, e). However, this concentration of S1P and dihydro-S1P, which is much greater than the dissociation constant ( $K_d$ ) values for the S1P receptors, activated ERK1/2 in these cells (Fig. 1b, f, g and Supplementary Fig. 6d), indicating that the lack of effect on the NF- $\kappa$ B pathway is not due to an inability of S1P to signal through its cell surface receptors. Moreover, the S1P<sub>1</sub> and S1P<sub>3</sub> antagonist VPC23019 did not affect TNF- $\alpha$ -induced phosphorylation of IKK and I $\kappa$ B $\alpha$  or its degradation in these cells (Supplementary Fig. 6e). Furthermore, in contrast to TNF- $\alpha$ , neither S1P nor dihydro-S1P stimulated NF- $\kappa$ B reporter activity (Fig. 1e). To corroborate the notion that the actions of SphK1 were due to intracellular-generated S1P, we took advantage of our previous observation that only high concentrations of exogenously added S1P significantly increase its intracellular levels<sup>12</sup>. Although S1P at 100 nM had no significant effects (Fig. 1e,f), treatment with 10  $\mu$ M S1P, which increased the total intracellular pools of S1P by sevenfold (Fig. 1h), enhanced the phosphorylation of IKK $\alpha$ / $\beta$  and I $\kappa$ B $\alpha$  (Fig. 1f, g) and NF- $\kappa$ B reporter activity (Fig. 1i). This high concentration of S1P also enhanced the response to a suboptimal dose of TNF- $\alpha$  (Fig. 1f, i). Notably, a high concentration of dihydro-S1P, which has the same rate of uptake as S1P<sup>13</sup> and increases its intracellular level to a similar or even greater extent (Fig. 1h), did not mimic the effects of S1P on activation of the

reporter activity was determined in A7 cells stimulated with TNF- $\alpha$ , 100 nM S1P or dihydro-S1P (DHS1P). \* $P$  < 0.01. **f**, A7 cells were stimulated with TNF- $\alpha$  (1 ng ml<sup>-1</sup>) or S1P (100 nM or 10  $\mu$ M) for 10 min. **g**, HeLa cells were stimulated with TNF- $\alpha$  (1 ng ml<sup>-1</sup>), 10  $\mu$ M S1P or dihydro-S1P. **h**, Sphingolipids were analysed by LC-ESI-MS/MS. \* $P$  < 0.01. **i**, NF- $\kappa$ B reporter activity was determined in HeLa cells stimulated with TNF- $\alpha$  (1 ng ml<sup>-1</sup>), S1P (10  $\mu$ M), or both. \* $P$  < 0.01 compared to 'none'.  $n$  = 3. Data are representative of two or more independent experiments and are means and s.d. of triplicates (**d**, **e**, **h**, **i**).

NF- $\kappa$ B pathway (Fig. 1g). Thus, intracellular S1P generated by the activation of SphK1 specifically regulates TNF- $\alpha$ -induced NF- $\kappa$ B in a S1P-receptor-independent manner.

Unlike Lys-48-linked polyubiquitination, which targets proteins for proteasomal degradation, abundant evidence has demonstrated that Lys-63-linked or regulatory ubiquitination has a critical role in signalling activation<sup>5</sup>. One of the best characterized examples is the non-degradative Lys 63 polyubiquitination of RIP1 that serves as a scaffold to recruit proteins containing specific ubiquitin binding domains, resulting in the recruitment and phosphorylation of the IKK complex, leading to the activation of NF- $\kappa$ B<sup>3,14,15</sup>. Figure 2a shows that the high molecular mass species of RIP1 rapidly formed in response to TNF- $\alpha$  were greatly diminished by depletion of SphK1. Analysis of immunoprecipitated RIP1 by immunoblotting with a ubiquitin-specific antibody verified that knockdown of SphK1 reduced polyubiquitination of RIP1 (Fig. 2b). Furthermore, siRNA targeting SphK1 (siSphK1) markedly reduced the TNF- $\alpha$ -induced conjugation of ectopically expressed ubiquitin with RIP1 (Fig. 2c). An antibody that specifically recognizes Lys-63-linked ubiquitin chains<sup>16</sup> revealed that endogenous Lys-63-linked polyubiquitination of RIP1 was stimulated by TNF- $\alpha$ , consistent with a previous study<sup>17</sup>, but this was greatly attenuated by SphK1 depletion (Fig. 2d). As was previously reported<sup>18–20</sup>, after TNF- $\alpha$  stimulation TRAF2 itself was polyubiquitinated and this was markedly reduced in cells depleted of SphK1 (Fig. 2e). Taken together, these results indicate that SphK1 and intracellularly generated S1P are important for Lys-63-linked polyubiquitination of RIP1, leading to recruitment and activation of the IKK complex.

Although it has been shown that RIP1 ubiquitination is dependent on TRAF2 expression<sup>3</sup>, evidence that TRAF2 directly catalyses the

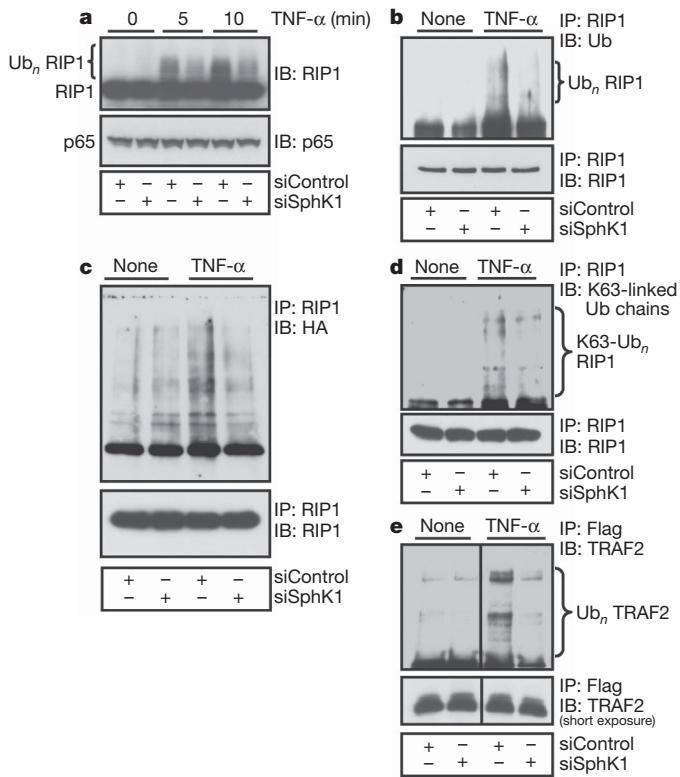


**Figure 2 | SphK1 is required for TNF- $\alpha$ -induced Lys-63-linked polyubiquitination of RIP1.** **a**, A7 cells transfected with siControl or siSphK1 were stimulated with TNF- $\alpha$  (10 ng ml $^{-1}$ ). Proteins were immunoblotted (IB) with anti-RIP1 or anti-p65 antibodies. **b**, Lysates were immunoprecipitated (IP) with anti-RIP1 antibody and analysed with anti-ubiquitin antibody. **c**, Lysates from cells transfected with haemagglutinin (HA)-Ub and stimulated with TNF- $\alpha$  were immunoprecipitated with anti-RIP1 antibody and analysed with HA antibody. **d**, Lysates were immunoprecipitated with anti-RIP1 antibody and proteins analysed with Lys-63-specific polyubiquitin antibody. **e**, HEK 293 cells transfected with siControl or siSphK1 were transfected with Flag-TRAF2 and stimulated with TNF- $\alpha$ . Proteins were pulled down with anti-Flag beads and analysed with anti-TRAF2 antibody.

ubiquitination of RIP1 is still lacking. Because intracellularly generated S1P was required for optimal TRAF2 and RIP1 polyubiquitination after stimulation by TNF- $\alpha$ , and SphK1 interacts with TRAF2<sup>4</sup>, we examined whether S1P is required for direct RIP1 ubiquitination by TRAF2 *in vitro*. In agreement with previous studies<sup>20,21</sup>, incubation of purified RIP1 with recombinant TRAF2, ubiquitin, the ubiquitin-activating enzyme E1, and Ubc13-Uev1a—an E2 that facilitates

Lys63 polyubiquitination—failed to produce ubiquitinated RIP1. However, addition of S1P induced efficient TRAF2-mediated ubiquitination of RIP1 (Fig. 3a). In contrast, dihydro-S1P did not mimic the effect of S1P (Fig. 3a). Neither sphingosine nor LPA, lipids structurally related to S1P, enhanced *in vitro* ubiquitination of RIP1 by TRAF2 (Supplementary Fig. 7a). Furthermore, TRAF2 with a deletion of the N-terminal 87 amino acids containing the RING domain (TRAF2( $\Delta$ RING)), which cripples its E3 ligase activity, failed to ubiquitinate RIP1 in the absence or presence of S1P (Fig. 3b, c), underscoring the importance of the E3 ligase activity of TRAF2. To determine whether the ubiquitin conjugated to RIP1 *in vitro* was Lys-63 linked, we examined TRAF2-mediated polyubiquitination of RIP1 with wild-type ubiquitin and its mutants containing only one lysine at either position 48 (Lys48) or 63 (Lys63). S1P enhanced incorporation of wild-type and Lys-63-only ubiquitin into RIP1, whereas there was little or no incorporation of the Lys-48-only mutant in the presence of S1P (Fig. 3b, c). Even with the promiscuous E2 enzyme Ubc5a, S1P was still capable of stimulating TRAF2-mediated polyubiquitination of RIP1 with wild-type and Lys-63-only ubiquitin but not with Lys-48-only ubiquitin. This effect was also dependent on the presence of the RING domain of TRAF2 (Fig. 3c).

Although TRAF2 can act as an adaptor for cIAP1 and cIAP2, which can themselves serve as E3 ligases for RIP1 (refs 21–23), neither cIAP1/2 nor TRAF5 were associated with purified TRAF2 used for *in vitro* ubiquitination assays (Supplementary Fig. 7b). Moreover, S1P also enhanced the E3 ligase activity of recombinant TRAF2 purified from Sf9 insect cells (Supplementary Fig. 7c), further demonstrating that TRAF2 itself is the target of S1P.

Because our results show that S1P is required for the *in vitro* E3 ligase activity of TRAF2, it was important to confirm that TRAF2 is a direct target of intracellularly produced S1P. To this end, we first examined binding of TRAF2 to S1P immobilized on agarose beads. Both ectopically expressed Flag-TRAF2 (Fig. 4a) and endogenous TRAF2 (Fig. 4b) were pulled down by matrices carrying S1P but not by control, sphingosine, or LPA matrices. Pre-incubation with exogenous S1P abolished binding of endogenous TRAF2 to the S1P affinity beads (Fig. 4b). Moreover, recombinant TRAF2 purified from Sf9 insect cells also bound to S1P beads, whereas RIP1 and TRAF2( $\Delta$ RING) did not (Supplementary Fig. 7d–f).

Next, direct binding of S1P to TRAF2 was evaluated. <sup>32</sup>P-labelled S1P specifically bound to Flag-tagged TRAF2 that was eluted from anti-Flag agarose beads with Flag peptide. Of note, binding to TRAF2 was abolished by addition of excess cold S1P but not by dihydro-S1P, LPA, or sphingosine (Fig. 4c), in agreement with the specific requirement for S1P to activate the E3 ligase activity of TRAF2 (Fig. 3a). Binding of <sup>32</sup>P-S1P to TRAF2 was reduced by 50% at a concentration of 0.5  $\mu$ M unlabelled S1P (Supplementary Fig. 8a). Finally, we sought

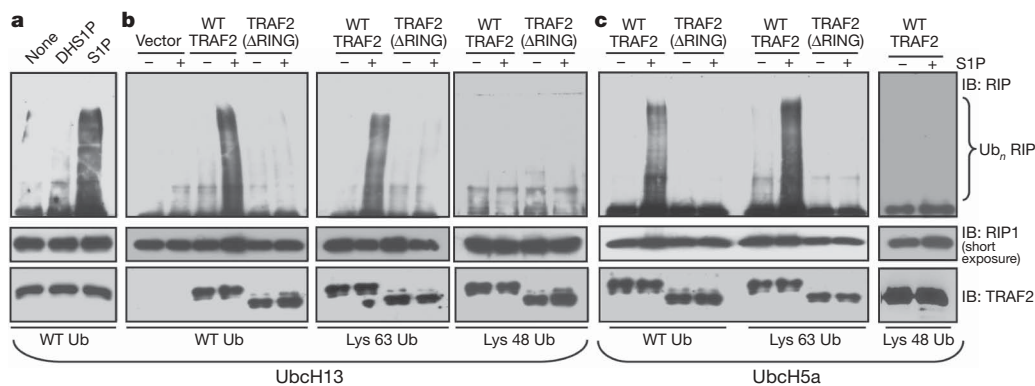


**Figure 3 | S1P is required for TRAF2-mediated Lys-63-linked polyubiquitination of RIP1 *in vitro*.** **a**, *In vitro* ubiquitination of purified RIP1 was carried out with ATP, E1, Ubc13-Uev1a, ubiquitin and TRAF2 with the indicated lipids (100 nM) and examined with anti-RIP1 antibody. **b, c**, Ubiquitination reactions were carried out with purified wild-type (WT)

TRAF2 or TRAF2( $\Delta$ RING) in the presence of UbcH13-Uev1a (**b**) or UbcH5a-Uev1a (**c**) as E2s and ubiquitin proteins (wild type, Lys 63 only, or Lys 48 only), without or with 100 nM S1P. RIP1 ubiquitination was determined with anti-RIP1 antibody and TRAF2 input with anti-TRAF2 antibody.



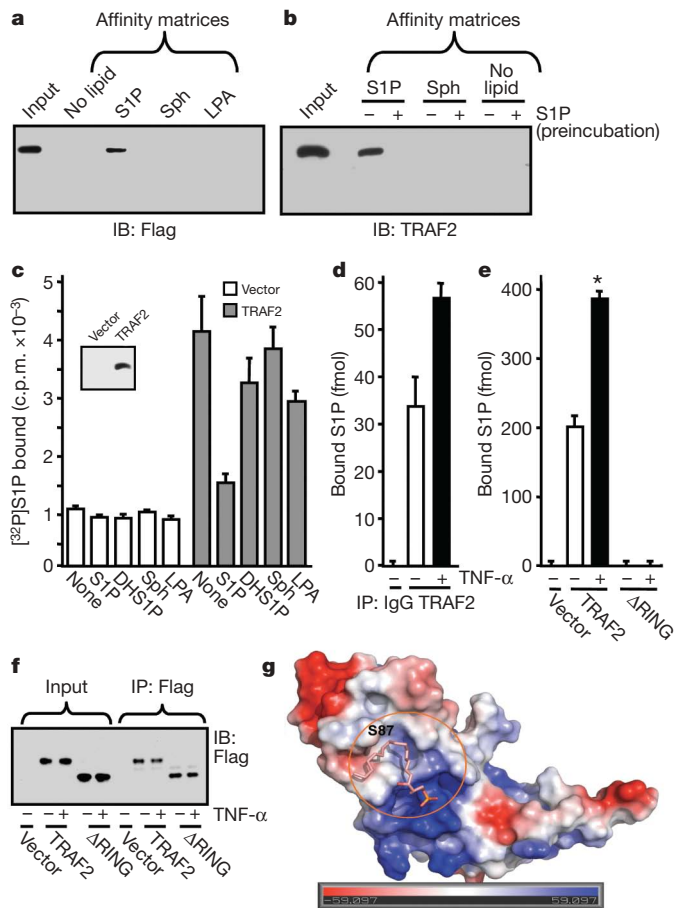


**Figure 4 | Specific binding of S1P to TRAF2.** **a**, Lysates from HEK 293 cells transfected with Flag-TRAF2 were incubated with control (no lipid), S1P, LPA, or sphingosine affinity matrices. **b**, Lysates from naive cells were pre-treated with 10  $\mu$ M S1P, followed by pull down with control (no lipid), S1P, or sphingosine affinity matrices and bound proteins analysed by immunoblotting. **c**, Lysates from vector or Flag-TRAF2-transfected cells were incubated with anti-Flag agarose beads. Beads were washed and incubated with [ $^{32}$ P]S1P (0.1 nM) in the absence or presence of 1  $\mu$ M unlabelled S1P, dihydro-S1P, sphingosine or LPA, and [ $^{32}$ P]S1P bound to TRAF2 was eluted with Flag peptide and radioactivity determined. The insert shows a blot of eluted TRAF2. c.p.m., counts per minute. **d**, Naive cells were stimulated with TNF- $\alpha$ . Lysates were immunoprecipitated with anti-TRAF2 antibody or control IgG and bound sphingolipids determined by LC-ESI-MS/MS. Of all of the sphingolipids present in these cells (Supplementary Table 1), only S1P was detected in the immunocomplexes. **e**, **f**, Cells transfected with vector, Flag-TRAF2, or Flag-TRAF2( $\Delta$ RING) were stimulated with TNF- $\alpha$ . Lysates were immunoprecipitated with anti-Flag antibody. **e**, Bound S1P determined by LC-ESI-MS/MS. **f**, Immunoblot with anti-Flag antibody. **g**, Docking of S1P into the pocket of the RING domain of TRAF2. Surface contour of the binding site with S1P was coloured by electrostatic potential. **c–e**, Data are means and s.d. of triplicates.

to examine whether endogenous S1P is bound to TRAF2 *in vivo* and whether this interaction is influenced by TNF- $\alpha$ , which activates SphK1. Cells were treated with TNF- $\alpha$  and the sphingolipids in TRAF2 immunoprecipitates were measured by liquid chromatography electrospray ionization tandem mass spectrometry (LC-ESI-MS/MS). Of all the sphingolipids present in cells, only S1P was bound to TRAF2 (Fig. 4d and Supplementary Table 1), and this association was significantly increased by TNF- $\alpha$  (Fig. 4d). Moreover, as expected from a specific interaction, much more S1P was bound to ectopically expressed TRAF2, and this association was further enhanced by treatment with TNF- $\alpha$ . However, there was no detectable S1P associated with TRAF2( $\Delta$ RING) as measured by LC-ESI-MS/MS (Fig. 4e,f), which also did not bind to S1P affinity beads

(Supplementary Fig. 7f), indicating that the binding site for S1P is within the RING domain of TRAF2.

Molecular modelling of S1P into the RING domain of the crystal structure of TRAF2 (ref. 24) revealed that it docked remarkably well in a 16- $\text{\AA}$ -long binding cavity consisting of a hydrophobic region (Phe 45, Leu 58, Ala 59, Leu 62, Ala 90, Phe 91 and Phe 92) and positively charged region (Arg 43 and Arg 97), which may stabilize the phosphate group of S1P (Fig. 4g and Supplementary Fig. 9). Further molecular dynamic simulation and free energy calculation indicates the binding for S1P is  $-8.07 \text{ kcal mol}^{-1}$  whereas dihydro-S1P shows instability in binding with TRAF2 during the dynamic simulation process, consistent with the inability of dihydro-S1P to bind or activate TRAF2. Indeed, estimated  $K_i$  values by AutoDock<sup>25</sup> for S1P and dihydro-S1P are  $8.74 \times 10^{-7}$  and  $5.37 \times 10^{-4}$ , respectively ( $T = 298.15 \text{ K}$ ). In contrast, no binding was detected to TRAF3 (Supplementary Fig. 8b, c). In agreement, sequence alignment and homology modelling did not identify an obvious binding pocket near residue Lys 97 of TRAF3 (corresponding to Ser 87 in TRAF2). S1P also stimulated *in vitro* auto-ubiquitination of recombinant TRAF2 (Supplementary Fig. 8d).

Hence, S1P is a missing cofactor for TRAF2, an E3 ligase that has an important role in Lys-63-linked polyubiquitination of RIP1 and consequent regulation of NF- $\kappa$ B activation and the antiapoptotic programme initiated by TNF- $\alpha$ <sup>1,2,5</sup>. Increased RIP1 Lys 63 ubiquitination prevents switching of RIP1 from a pro-survival to pro-apoptotic adaptor protein (Supplementary Fig. 10). These findings also resolve the puzzle associated with the cytoprotective effects of SphK1 and S1P<sup>7</sup>. Although S1P and dihydro-S1P are equally potent ligands for the five S1P receptors, only S1P suppresses apoptosis as only S1P, and not dihydro-S1P, binds to and activates TRAF2. Our study also provides a mechanistic explanation for the numerous observations of the importance of SphK1 in inflammatory, antiapoptotic and immune processes.

## METHODS SUMMARY

For details of expression plasmids, proteins, antibodies, cell lines and methods for immunoprecipitations, immunofluorescence, pull downs, S1P binding and mass spectrometry, see Methods. *In vitro* ubiquitination assays were performed as described previously<sup>22</sup>, with some modifications, as described in Methods.

**Full Methods** and any associated references are available in the online version of the paper at [www.nature.com/nature](http://www.nature.com/nature).

Received 11 November 2009; accepted 26 April 2010.

- Karin, M. & Gallagher, E. TNFR signaling: ubiquitin-conjugated TRAF signals control stop-and-go for MAPK signaling complexes. *Immunol. Rev.* **228**, 225–240 (2009).
- Hayden, M. S. & Ghosh, S. Shared principles in NF- $\kappa$ B signaling. *Cell* **132**, 344–362 (2008).
- Lee, T. H., Shank, J., Cusson, N. & Kelliher, M. A. The kinase activity of Rip1 is not required for tumor necrosis factor- $\alpha$ -induced I $\kappa$ B kinase or p38 MAP kinase activation or for the ubiquitination of Rip1 by Traf2. *J. Biol. Chem.* **279**, 33185–33191 (2004).
- Xia, P. *et al.* Sphingosine kinase interacts with TRAF2 and dissects tumor necrosis factor- $\alpha$  signaling. *J. Biol. Chem.* **277**, 7996–8003 (2002).
- Bhoj, V. G. & Chen, Z. J. Ubiquitylation in innate and adaptive immunity. *Nature* **458**, 430–437 (2009).
- Paugh, S. W. *et al.* A selective sphingosine kinase 1 inhibitor integrates multiple molecular therapeutic targets in human leukemia. *Blood* **112**, 1382–1391 (2008).
- Spiegel, S. & Milstien, S. Sphingosine-1-phosphate: an enigmatic signalling lipid. *Nature Rev. Mol. Cell Biol.* **4**, 397–407 (2003).
- Kimura, T. *et al.* Role of scavenger receptor class B type I and sphingosine 1-phosphate receptors in high-density lipoprotein-induced inhibition of adhesion molecule expression in endothelial cells. *J. Biol. Chem.* **281**, 37457–37467 (2006).
- Ki, S. H., Choi, M. J., Lee, C. H. & Kim, S. G. G $\alpha_{12}$  specifically regulates COX-2 induction by sphingosine 1-phosphate: Role of JNK-dependent ubiquitination and degradation of I $\kappa$ B $\alpha$ . *J. Biol. Chem.* **282**, 1938–1947 (2007).
- Pitson, S. M. *et al.* Activation of sphingosine kinase 1 by ERK1/2-mediated phosphorylation. *EMBO J.* **22**, 5491–5500 (2003).
- Zhao, Y. *et al.* Intracellular generation of sphingosine 1-phosphate in human lung endothelial cells: Role of lipid phosphate phosphatase-1 and sphingosine kinase 1. *J. Biol. Chem.* **282**, 14165–14177 (2007).

12. Van Brocklyn, J. R. *et al.* Dual actions of sphingosine-1-phosphate: extracellular through the G<sub>i</sub>-coupled orphan receptor edg-1 and intracellular to regulate proliferation and survival. *J. Cell Biol.* **142**, 229–240 (1998).
13. Giussani, P. *et al.* Sphingosine-1-phosphate phosphohydrolase regulates endoplasmic reticulum-to-Golgi trafficking of ceramide. *Mol. Cell. Biol.* **26**, 5055–5069 (2006).
14. Ea, C. K., Deng, L., Xia, Z. P., Pineda, G. & Chen, Z. J. Activation of IKK by TNF $\alpha$  requires site-specific ubiquitination of RIP1 and polyubiquitin binding by NEMO. *Mol. Cell* **22**, 245–257 (2006).
15. Wu, C. J., Conze, D. B., Li, T., Srinivasula, S. M. & Ashwell, J. D. Sensing of Lys-63-linked polyubiquitination by NEMO is a key event in NF- $\kappa$ B activation. *Nature Cell Biol.* **8**, 398–406 (2006).
16. Wang, H. *et al.* Analysis of nondegradative protein ubiquitylation with a monoclonal antibody specific for lysine-63-linked polyubiquitin. *Proc. Natl Acad. Sci. USA* **105**, 20197–20202 (2008).
17. Newton, K. *et al.* Ubiquitin chain editing revealed by polyubiquitin linkage-specific antibodies. *Cell* **134**, 668–678 (2008).
18. Shi, C. S. & Kehrl, J. H. Tumor necrosis factor (TNF)-induced germinal center kinase-related (GCKR) and stress-activated protein kinase (SAPK) activation depends upon the E2/E3 complex Ubc13-Uev1A/TNF receptor-associated factor 2 (TRAF2). *J. Biol. Chem.* **278**, 15429–15434 (2003).
19. Habelhah, H. *et al.* Ubiquitination and translocation of TRAF2 is required for activation of JNK but not of p38 or NF- $\kappa$ B. *EMBO J.* **23**, 322–332 (2004).
20. Li, S., Wang, L. & Dorf, M. E. PKC phosphorylation of TRAF2 mediates IKK $\alpha$ / $\beta$  recruitment and K63-linked polyubiquitination. *Mol. Cell* **33**, 30–42 (2009).
21. Bertrand, M. J. *et al.* cIAP1 and cIAP2 facilitate cancer cell survival by functioning as E3 ligases that promote RIP1 ubiquitination. *Mol. Cell* **30**, 689–700 (2008).
22. Varfolomeev, E. *et al.* c-IAP1 and c-IAP2 are critical mediators of tumor necrosis factor  $\alpha$  (TNF $\alpha$ )-induced NF- $\kappa$ B activation. *J. Biol. Chem.* **283**, 24295–24299 (2008).
23. Xu, M., Skaug, B., Zeng, W. & Chen, Z. J. A ubiquitin replacement strategy in human cells reveals distinct mechanisms of IKK activation by TNF $\alpha$  and IL-1 $\beta$ . *Mol. Cell* **36**, 302–314 (2009).
24. Yin, Q., Lamothe, B., Darnay, B. G. & Wu, H. Structural basis for the lack of E2 interaction in the RING domain of TRAF2. *Biochemistry* **48**, 10558–10567 (2009).
25. Morris, G. M. *et al.* Automated docking using a Lamarckian genetic algorithm and empirical binding free energy function. *J. Comput. Chem.* **19**, 1639–1662 (1998).

**Supplementary Information** is linked to the online version of the paper at [www.nature.com/nature](http://www.nature.com/nature).

**Acknowledgements** We thank Z. J. Chen, B. Darnay and M. Karin for HA-ubiquitin and TRAF constructs, and R. Proia for the *Sphk1*<sup>-/-</sup> mice. This work was supported by grants from the National Institute of Health (R37GM043880, R01CA61774, R01AI50094, U19AI077435 to S.S.) and in part by the Ministry of Scientific and Technology of China (2009CB918502 to C.L.).

**Author Contributions** S.E.A. and K.B.H. planned and performed most experiments, with assistance from N.C.H., G.M.S., E.Y.K., J.A. and M.M.; C.L. and H.J. performed molecular docking; T.K. contributed to the planning of the experiments; S.M. and S.S. conceived the study, contributed to planning of the experiments and wrote the manuscript.

**Author Information** Reprints and permissions information is available at [www.nature.com/reprints](http://www.nature.com/reprints). The authors declare no competing financial interests. Readers are welcome to comment on the online version of this article at [www.nature.com/nature](http://www.nature.com/nature). Correspondence and requests for materials should be addressed to S.S. ([sspiegel@vcu.edu](mailto:sspiegel@vcu.edu)).

## METHODS

**Reagents and antibodies.** S1P, SKI-1 ((2R,3S,4E)-*N*-methyl-5-(4'-pentylphenyl)-2-aminopent-4-ene-1,3-diol) and mouse monoclonal polyubiquitin (K63-linkage specific) antibody were obtained from Enzo Life Sciences International. Other lipids and VPC23019 were from Avanti Polar Lipids. Wild-type and Lys mutant ubiquitins were from Boston Biochem. Antibodies against the following were used for immunoblotting: p65, I $\kappa$ B $\alpha$ , I $\kappa$ B $\beta$ , IKK $\alpha$  and IKK $\beta$ , ubiquitin, TRAF3, TRAF5 and ERK2 (Santa Cruz Biotechnology); phospho-p65 (Ser 536), phospho-I $\kappa$ B $\alpha$  (Ser 32), phospho-p44/42 ERK1/2 (Thr 202/Tyr 204), phospho-IKK $\alpha$ / $\beta$  (Ser 176/180), phospho-JNK (Thr 183/Tyr 185), phospho-p38 (Thr 180/Tyr 182), His-tag, tubulin and TRAF2 (Cell Signaling); RIP1 (BD Transduction Laboratories). Rabbit polyclonal SphK1 and SphK2 antibodies were described previously<sup>26</sup> and rabbit polyclonal SphK1 (Ser 225) phospho-specific antibody was from ECM Biosciences. Mouse anti-human CD40 antibody was provided by D. Conrad. Expression plasmids for wild-type TRAF2, Flag-TRAF2( $\Delta$ RING) with 87 amino acids deleted from the N terminus including the RING domain, and Flag-TRAF3 were provided by B. Darnay (wild-type TRAF2 and Flag-TRAF2( $\Delta$ RING)) and M. Karin (Flag-TRAF3).

**Cell culture and transfections.** A7 melanoma cells, FM-516 normal immortal melanocytes, HeLa, HEK 293 and RPMI-8866 cells were cultured as described<sup>27</sup>. MEFs were isolated from E14 wild-type or *Sphk1*<sup>-/-</sup> embryos<sup>28</sup>. Cells were serum-starved overnight and then stimulated with TNF- $\alpha$  (10 ng ml<sup>-1</sup>) for 10 min unless indicated otherwise. Cells were transfected with Lipofectamine Plus or GeneJuice for plasmids or Oligofectamine for siRNA. SphK1 and SphK2 were downregulated with sequence-specific siRNA from Qiagen as previously described<sup>26</sup>. In some experiments, to confirm lack of off-target effects, cells were transfected with individual ON-TARGETplus SMARTpool siRNAs targeted to other SphK1 sequences (5'-GAAUCUCCUACGCUGA-3' and 5'-GGAAAGGUGUGUU UGCAGU-3') and control siRNA (Dharmacon).

**SphK1 activity.** SphK1 activity was determined exactly as described<sup>27</sup>.

**RIP1 immunoprecipitation.** Cell extracts were prepared in HEPES 20 mM pH 7.4 containing 150 mM NaCl, 10 mM  $\beta$ -glycerophosphate, 1.5 mM MgCl<sub>2</sub>, 10 mM NaF, 2 mM dithiothreitol, 1 mM sodium orthovanadate, 2 mM EGTA, 1 mM PMSF, 0.5% Triton X-100, 1:500 protease inhibitor cocktail (Sigma-Aldrich), and 1 mg ml<sup>-1</sup> of *N*-ethylmaleimide. RIP1 was immunoprecipitated from 200  $\mu$ g of cell lysate with 1  $\mu$ g anti-RIP antibody overnight at 4 °C. Immunoprecipitates were captured with protein A/G-plus agarose beads (Santa Cruz). After extensive washing, bound proteins were released by boiling in SDS-PAGE sample buffer and polyubiquitination of RIP1 determined by western blotting.

**Electrophoretic mobility shift assays.** Electrophoretic mobility shift assays were performed with 5  $\mu$ g of nuclear protein and [ $\alpha$ -<sup>32</sup>P]dCTP-end-labelled double-strand oligonucleotides containing an NF- $\kappa$ B consensus binding site (10 fmol, 10,000 c.p.m.) exactly as described<sup>29</sup>.

**NF- $\kappa$ B reporter assays.** Cells were transiently transfected with NF- $\kappa$ B-luciferase and RSV- $\beta$ -galactosidase or Renilla reporter plasmids using GeneJuice (EMD Biosciences). Forty-eight hours later, cells were stimulated with TNF- $\alpha$  for 18 h and combined measurements of luciferase and  $\beta$ -galactosidase activities determined with the Dual-Light chemiluminescent reporter gene assay (Applied Biosystems). Reporter activity was expressed as relative luciferase units normalized to  $\beta$ -galactosidase or Renilla activity.

**Immunofluorescence.** Cells grown on coverslips were fixed with 3% paraformaldehyde for 20 min, washed extensively, quenched by addition of 10 mM glycine in PBS, and permeabilized with 0.5% Triton X-100 for 3 min. After incubation with primary and appropriate fluorescent secondary antibodies (Molecular Probes), coverslips were mounted on slides with 10 mM *n*-propylgallate in 100% glycerol and visualized with a Zeiss LSM 510 laser confocal microscope. ImageJ version 1.6.0\_12 image analysis software was used for computerized quantification of p65 nuclear fluorescence staining as described<sup>30</sup>.

**In vitro ubiquitination and protein purification.** Ubiquitination assays were performed as described<sup>22</sup>, with some modifications. Flag-tagged TRAF2 was purified from HEK 293 overexpressing cells with anti-Flag M2 affinity beads and eluted with Flag peptide (Sigma). His-tagged TRAF2 purified from Sf9 cells

(Signal Chem) was used as the E3 ligase in some experiments. RIP1 was immunocaptured from A7 cells. Ubiquitination assays were carried out at 35 °C for 2 h in 50 mM HEPES, pH 7.8, containing 5 mM MgCl<sub>2</sub>, 4 mM ATP, 50 nM E1, 10  $\mu$ g ubiquitin (wild type, Lys48 only or Lys63 only), 150 nM UbcH5-Uev1a or UbcH13-Uev1a E2 complexes (Boston Biochem), and purified Flag-TRAF2 and RIP1 bound to agarose beads, in the absence or presence of various lipids. Reactions were stopped by boiling in SDS sample buffer, proteins resolved by SDS-PAGE, and immunoblotted. *In vitro* autoubiquitination reactions were carried out with purified recombinant His-TRAF2 captured on beads in the presence of ATP, ubiquitin and UbcH13-Uev1a as described above.

**Pull downs with lipid affinity matrices.** Control, S1P-, sphingosine- and LPA-coated agarose beads (Echelon Biosciences) equilibrated with binding buffer containing 10 mM HEPES (pH 7.8), 150 mM NaCl, 1:500 protease inhibitor cocktail, and 0.5% Igepal were mixed with cell extracts diluted in binding buffer and rocked for 2 h at 4 °C. Beads were washed four times with binding buffer and collected by centrifugation at 1,000 r.p.m. After removing the supernatant, the beads were boiled in SDS-PAGE sample buffer and bound proteins analysed by immunoblotting.

**Quantification of S1P by mass spectrometry.** Cell extracts (500  $\mu$ g) were immunoprecipitated with anti-TRAF2 or anti-Flag antibodies, or control IgG. Lipids were extracted, and sphingolipids quantified by liquid chromatography, electrospray ionization-tandem mass spectrometry (LC-ESI-MS/MS, 4000 QTRAP, ABI) as described<sup>26</sup>.

**[<sup>32</sup>P]S1P binding assays.** Cells overexpressing Flag-tagged TRAF proteins or empty vector were lysed by freeze-thawing in buffer containing 50 mM Tris (pH 7.4), 150 mM NaCl, 1 mM EDTA, 0.5% NP-40 and 1:500 protease inhibitor cocktail. Lysates (400  $\mu$ g) were incubated with 150  $\mu$ l anti-Flag antibody-conjugated agarose beads (Sigma-Aldrich) overnight at 4 °C with agitation. The beads were then washed extensively and incubated without or with unlabelled lipids in the presence of [<sup>32</sup>P]S1P (0.1 nM, 6.8  $\mu$ Ci pmol<sup>-1</sup>) in 150  $\mu$ l buffer containing 50 mM Tris (pH 7.5), 137 mM NaCl, 1 mM MgCl<sub>2</sub>, 2.7 mM KCl, 15 mM NaF, 0.5 mM NaV<sub>3</sub>O<sub>4</sub> for 60 min at 4 °C. Bound TRAF proteins were eluted with 40  $\mu$ l Flag peptide (250  $\mu$ g ml<sup>-1</sup>). [<sup>32</sup>P]S1P bound to the eluted proteins was quantified with a LS6500 scintillation counter (Beckman). S1P binding to His-tagged TRAF proteins was measured as described<sup>26</sup>.

**Molecular docking, MD simulation and free energy calculation.** The molecular docking program AutoDock 4.0 was used for the automated molecular docking simulations<sup>25</sup>. Briefly, the PDBQT file was created and the AutoGrid algorithm and the Kollman all-atom charges were assigned for TRAF2 and Gasteiger-Marsili charges were assigned for the ligands. Complexes were selected according to the criteria of interacting energy combined with geometrical matching quality. These complexes were subjected to molecular dynamic simulations by AMBER9.0 software package solvated using a box of TIP3P water molecules extending at least 10 Å away from the boundary of any protein atoms. The MM\_PBSA and Nmode module of AMBER program were used for the free energy calculation of the TRAF2-S1P complex.

**Statistical analysis.** All experiments were repeated at least three times with consistent results. Data are means  $\pm$  s.d. Statistical significance was assessed by two-tailed unpaired student's *t*-test. *P* < 0.05 was considered significant.

26. Hait, N. C. *et al.* Regulation of histone acetylation in the nucleus by sphingosine-1-phosphate. *Science* **325**, 1254–1257 (2009).
27. Maceyka, M., Alvarez, S. E., Milstien, S. & Spiegel, S. Filamin A links sphingosine kinase 1 and sphingosine-1-phosphate receptor 1 at lamellipodia to orchestrate cell migration. *Mol. Cell. Biol.* **28**, 5687–5697 (2008).
28. Allende, M. L. *et al.* Mice deficient in sphingosine kinase 1 are rendered lymphopenic by FTY720. *J. Biol. Chem.* **279**, 52487–52492 (2004).
29. Paugh, B. S. *et al.* EGF regulates plasminogen activator inhibitor-1 (PAI-1) by a pathway involving c-Src, PKC $\delta$ , and sphingosine kinase 1 in glioblastoma cells. *FASEB J.* **22**, 455–465 (2008).
30. Theiss, A. L. *et al.* Prohibitin inhibits tumor necrosis factor  $\alpha$ -induced nuclear factor- $\kappa$ B nuclear translocation via the novel mechanism of decreasing importin  $\alpha$ 3 expression. *Mol. Biol. Cell* **20**, 4412–4423 (2009).